Regional Differences and Metabolic Changes in Normal Aging of the Human Brain: Proton MR Spectroscopic Imaging Study

Emmanuelle Angelie, Alain Bonmartin, Abdel Boudraa, Pierre-Marie Gonnaud, Jean-Jacques Mallet, and Dominique Sappey-Marinier

BACKGROUND AND PURPOSE: **Aging is recognized to originate from a diversity of mechanisms that blur the limits between normal and pathologic processes. The purpose of this study was to determine the early effect of normal aging on the regional distribution of brain metabolite concentrations, including *N*-acetylaspartate (NAA), a major neuronal marker, choline (Cho), and creatine (Cr).**

METHODS: **Thirty-two healthy participants, ages 21 to 61 years, were examined by proton MR spectroscopic (^{1}H MRS) imaging. ^{1}H MRS imaging acquisitions were performed in two brain locations: the centrum semiovale and the temporal lobe. Thirty voxels were selected in four cerebral regions, cortical, semioval, temporal, and hippocampal, and ^{1}H MR spectra were processed to determine the metabolite ratios.**

RESULTS: **With advancing age of the participants, the ratios of %NAA, NAA:Cho, and NAA:Cr were significantly decreased, whereas the ratios of %Cho and %Cr were significantly increased in the cortical, semioval, and temporal regions. On the basis of the significant metabolic difference determined by cluster analysis, two groups of 16 participants with ages ranging from 21 to 39 years (younger group) and 40 to 61 years (older group) were compared. Repeated measures analysis of variance tests, with multiple comparison procedures between the two age groups and among the four brain region groups, showed significant decreases of the %NAA, NAA:Cho, and NAA:Cr ratios in the semioval and temporal regions of the older group compared with the younger group. When compared with other cerebral regions, %NAA and %Cho ratios were significantly decreased in the hippocampal and cortical regions, respectively.**

CONCLUSION: **These metabolic changes suggest that brain aging is characterized by a reduction in neuronal viability or function associated with an accelerated membrane degradation and/or an increase in glial cell numbers.**

Aging is recognized to originate from a diversity of mechanisms that blur the limits between normal and pathologic processes (1). Normal aging has

been associated with some degree of neuron and volume loss, accompanied by increasing adjacent glial cells (2). Recent studies have suggested that these changes are quantitatively less than previously thought and that they seem to be attributable to reductions of neuronal cell size rather than neuronal cell number (3). Furthermore, it is thought that the cognitive impairment associated with normal aging is due to neuronal dysfunction rather than to loss of neurons or synapses. The decline in levels of synaptic proteins involved in structural plasticity of axons and dendrites has suggested that disturbed mechanisms of plasticity may contribute to cognitive dysfunction during aging (4). Although these histologic features cannot be observed noninvasively, quantitative analysis of cerebral structures with volumetric MR imaging has indicated a progressive reduction in cerebral hemispheres (2–3.5% per decade) and an increase in ventricular volumes

(2% per decade) (5–8). T2-weighted MR images have also shown the presence of characteristic white matter hyperintensities in the elderly (9). Although these anatomic and radiographic features are often correlated with cognitive impairment (9, 10), it is unclear whether neuronal function declines with age in healthy people. A number of metabolic studies using positron emission tomography have shown a gradual decline in regional cerebral blood flow of gray and white matter (11–13), particularly of the frontal lobes (14). Whether these results reflect a decline in metabolic activity, a fall in the number of active neurons, or a reduction in neuron density remains uncertain.

Proton MR spectroscopy (^{1}H MRS) has the potential to detect and quantify different amino acids and metabolites of the human brain, including *N*-acetylaspartate (NAA), total creatine (Cr), and choline (Cho) compounds. Previous localized ^{1}H MRS studies have examined age-related changes of brain metabolite concentrations with a number of different methods, population size, and variable results (15–19). Because NAA has been shown to decrease dramatically in cases of neuronal disease (20–23), to be neuronal in origin and not present in mature glial cells (24), it may be used to evaluate neuronal viability. Some workers reported that NAA was reduced with respect to age in basal ganglia or in white and gray matter (25), whereas others have shown no age-related change in NAA. Cho-containing compounds, including phosphorylcholine and glycerophosphorylcholine, as precursor and breakdown products of membrane phospholipids, respectively, have been shown to increase with age in several brain regions (26). Total Cr concentration, which indicates the energetic metabolism of neurons and glia, has been shown to increase in parietal white matter in the persons older than 60 years. This last report confirmed the previous finding of an increase of phosphocreatine content with advancing age (27). However, these single-voxel studies are limited in the context of clinical spectroscopy to few brain locations that are of relatively large size. In contrast, imaging has significant advantages in terms of spatial resolution, efficiency of data acquisition, and mapping the distribution of cerebral metabolite levels. The results obtained in ^{1}H MRS imaging investigations of normal aging were also variable (28–30). No age-related changes in NAA concentration with increased concentrations in Cho only or in Cho and Cr were reported in gray and white matter. In contrast, metabolite ratios of NAA:Cr and NAA:Cho have been reported to decrease in cortical gray matter but not in white matter regarding age. These ^{1}H MRS imaging studies have suggested that metabolite concentrations of normal brain may vary depending on brain structures or tissues (31–33). However, most of them were performed in brain regions that are not particularly known for involvement in cognitive impairment with aging.

The present study investigated whether metabolic measurements can change in normal brain during the early period of aging, ranging from 21 to 61 years. To test this hypothesis, the metabolite distribution was determined by using ^{1}H MRS imaging in two brain locations that are most involved in neurodegenerative disorders and cognitive impairments. The first region of interest was centered at the centrum semiovale, including both gray and white matter, and the second was placed in the temporal lobe, including temporal white matter and hippocampal formations.

Methods

Participants and Neuropsychological Evaluation

Thirty-two healthy volunteers (17 women and 15 men), aged 21 to 61 years (mean age, 38 years), with university levels of education provided their informed consent to participate in this study. Volunteers were screened for histories of pacemaker use, diabetes, stroke, coronary artery disease, renal failure, liver failure, alcohol abuse, and psychiatric illness. All participants received a neuropsychological workup, including a Mini-Mental State Examination (34) and a battery of tests such as attention, motor function, sensitivity, memory, and language tests and visuoconstructive tasks. None of the participants were excluded for dementia (mean Mini-Mental State Examination score, 29.3; range, 28–30) or for history of neurologic or psychiatric illness. None had undergone or was undergoing any therapeutic treatment.

MR Examination

MR imaging and spectroscopic investigations were performed using a whole-body Philips system (Gyroscan ACS II) operating at 1.5 T and equipped with a quadrature head coil. Sagittal T1-weighted standard spin-echo sequences were obtained with imaging parameters of 600/30/1 (TR/TE/excitations). Two series of axial T2-weighted images were obtained using turbo spin-echo sequences with imaging parameters of 2900/120/1 and a turbo factor of 16. Centered at the centrum semiovale, 15 sections were acquired along the anterior commissure-posterior commissure axis, and seven sections were obtained from the temporal lobe along the hippocampal axis. Both T1- and T2-weighted images were obtained with a section thickness of 5 mm, an intersection gap of 0.5 mm, a field of view of 256 mm, and a matrix size of 256 × 256. These MR images were used to visualize any white matter hyperintensities and guide the MRS imaging localization. MR images were interpreted by a radiologist, and no white matter hyperintensities were observed.

^{1}H MRS imaging data sets were acquired using a spin-echo sequence with imaging parameters of 1500/272/1 and preselection of regions of interest (point-resolved spectroscopy sequence [PRESS] volume) (Fig 1). MRS images were phase-encoded over a field of view of 256 mm with a 32 × 32 rectangular sampling array, resulting in a nominal voxel resolution of 1.28 mL. The spectral sweep width was 2000 Hz. Water suppression was provided by a chemical shift select sequence with a selective pulse of 120 Hz bandwidth. In both acquisitions, unsuppressed water MRS imaging was recorded with 16 × 16 phase-encoding steps.

The first PRESS volume (13 × 10 × 2 cm³) was placed immediately above the corpus callosum along the anterior commissure-posterior commissure direction to encompass the semioval white matter and the cortical gray matter (Fig 1A–C). Extracranial lipid signal was attenuated by the use of a water eliminated Fourier transform sequence with a selective inversion pulse (bandwidth of 50 Hz and frequency offset at
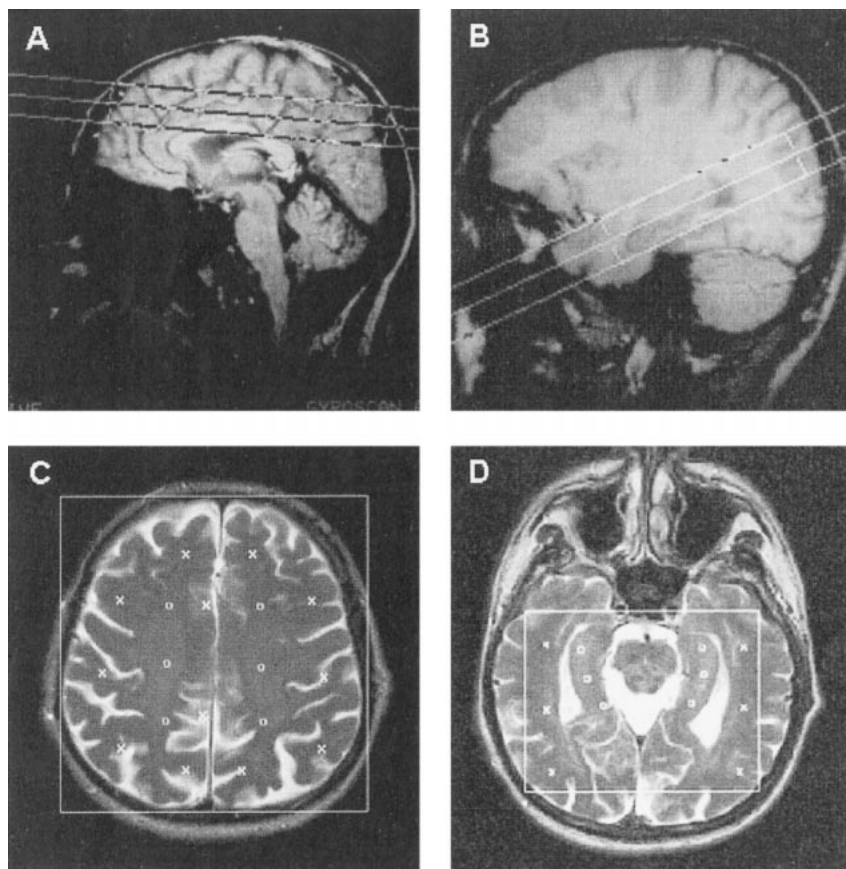
FIG 1. MR images identify the position of the PRESS volumes centered at the centrum semiovale and temporal lobe.

A, Sagittal T1-weighted MR image shows the PRESS volume (*large box*) localized at the centrum semiovale.

B, Sagittal T1-weighted MR image shows the PRESS volume (*large box*) localized in the temporal lobe.

C, Axial T2-weighted MR image shows the PRESS volume (*large box*) localized at the centrum semiovale. For metabolite quantitation, 30 voxels were selected and registered on the corresponding MR spectroscopic images. Markers indicate the positions of individual voxels selected in the cortical (*x*) and semioval (*o*) regions.

D, Axial T2-weighted MR image shows the PRESS volume (*large box*) localized in the temporal lobe. For metabolite quantitation, 30 voxels were selected and registered on the corresponding MR spectroscopic images. Markers indicate the positions of individual voxels selected in the temporal (*x*) and hippocampal (*o*) regions.

–225 Hz from the water peak) and an inversion time minimized to 304 ms (35). The second PRESS volume ($10 \times 10 \times 2$ cm^3) was placed in the temporal lobe along the hippocampal axis (Fig 1B–D). After MRS imaging acquisitions, two packages of three axial (6-mm thickness, 0.6-mm intersection gap) T2-weighted sections were collected with the coordinates of the MR spectroscopic images, using the above-described turbo spin-echo sequence (Fig 1C and D).

MRS Imaging Processing

All the raw data were transferred to a workstation (SUN, Ultra Sparc 1) and processed with a home-written subroutine using Interactive Data Language software. The unsuppressed water raw data were used to correct any frequency shifts due to magnetic susceptibility effects (36). The water-suppressed data were processed using a gaussian line broadening (3 Hz) to enhance the signal-to-noise ratio. A data shift accumulation (DSA) process of four points was applied to reduce the residual water peak (37). A sine window smoothing was used in both k-space directions, increasing the voxel size from 1.28 to 2 mL. MRS images were reconstructed by integrating the magnitude spectrum over a region of 20 Hz for NAA and 15 Hz for Cr and Cho peaks.

To determine whether there were regional differences in metabolite values, 30 individual voxels were selected in four regions: cortical, semioval, temporal, and hippocampal (Fig 1C and D). Placed on T2-weighted images, the voxel positions were registered on the spectroscopic images to extract the ^{1}H MR spectra. Twelve spectra were selected in the cortical region (prefrontal, frontal, frontoparietal, parietal, and occipital in each hemisphere and interhemispheric anterior and posterior). Six spectra were selected in the semioval, temporal, and hippocampal regions (anterior, middle, and posterior in each hemisphere).

The magnitude spectra were processed automatically using baseline correction and curve-fitting procedures to determine the resonance areas of NAA, Cho, and Cr. The baseline correction program consisted of two processes. For the first process, peaks were automatically detected by measuring consistent (>5 points) changes of the derivative sign, above a threshold fixed by the operator, and then subtracted from the spectrum. For the second process, residual baseline (after peak subtraction) was adjusted by minimizing the difference between the experimental data and a sinusoidal model function, which was previously defined to fit the baseline form modified by the DSA filter. Three gaussian line shape peaks were automatically fitted to the three selected peaks by using the gaussian function program provided by Interactive Data Language. Supervised by the operator, the fitting process was usually achieved after fewer than 10 iterations.

Individual signal integrals were used to calculate metabolite ratios (NAA:Cho, NAA:Cr, and Cho:Cr) and percentages (%metabolite is defined as the signal intensity integral of the metabolite divided by the sum of all metabolite signal intensity integrals). Because no significant differences between right and left hemispheres were detected by the repeated measures analysis of variance, these values were averaged and six metabolite measures were obtained for each cerebral region.

Because the DSA filter introduced a sinusoidal modification of the spectrum baseline, the effect on resonance intensities was determined experimentally by subtracting two spectra processed with and without DSA and by simulation. These results were used in this study to correct each metabolite ratio. %NAA, %Cr, and %Cho ratios were divided by 1.72, 1.14, and 1.04, respectively, and NAA:Cho, NAA:Cr, and Cho:Cr ratios were divided by 1.65, 1.51, and 0.91, respectively.

Statistical Analysis

Mean values and standard errors of six metabolite measures (%NAA, %Cho, %Cr, NAA:Cho, NAA:Cr, and Cho:Cr) were

FIG 2. Spectroscopic images of NAA obtained from the brain of a young participant. Four representative ^{1}H MR spectra (C1–C4) were selected from the voxels (voxels 1–4) in the cortical (C1), semioval (C2), hippocampal (C3), and temporal (C4) regions to illustrate the regional variations. The nominal size (0.8 × 0.8 × 2 cm³) of the individual voxels is shown on the MRS images.

A, Localized at the centrum semiovale.

B, Localized in the temporal lobe.
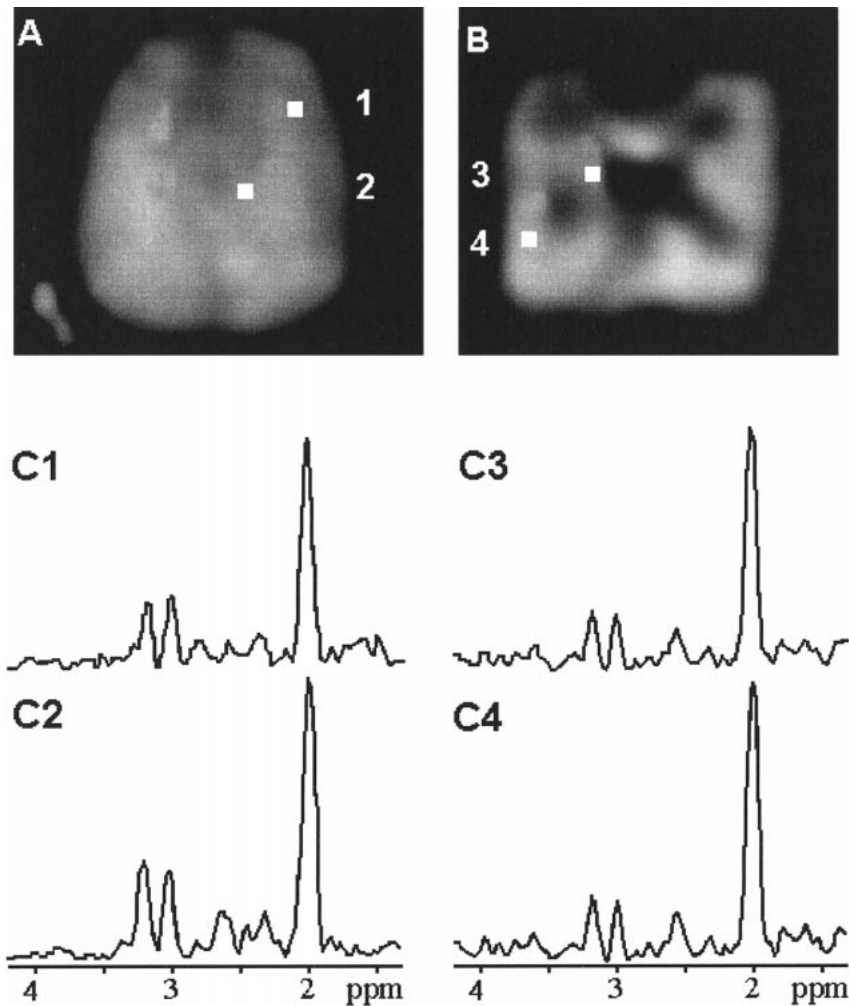
computed in four regions (cortical, semioval, temporal, and hippocampal) for each group. Data are reported as mean ± SD. Statistical analyses were performed using Sigmastat and Systat softwares.

Based on the significant results of cluster analysis using the k-means clustering algorithm (38), the participants were divided into two groups of 16 participants of ages ranging from 21 to 39 years (younger group) and 40 to 61 years (older group). To determine whether there were systematic differences in metabolite measures between hemispheres (left and right), among regions (cortical, semioval, temporal, and hippocampal), or by gender or age (younger and older), repeated measures analysis of variance was performed. The dependent variables were the six metabolite measures (%NAA, %Cho, %Cr, NAA:Cho, NAA:Cr, and Cho:Cr). Brain hemispheres, gender, and age were grouping variables, and region was a covariant (thus, these analyses adjusted for regional differences). To isolate which group differs from the others, a multiple comparison with Bonferroni's correction was performed. These age groups were then compared for each metabolite measure in each region by using a follow-up *t* test. Standard correlation and linear regression were performed to study the relationship between the metabolite measures and the age of the participants. *P* < .05 was considered statistically significant.

Results

Figure 1 shows sagittal T1-weighted and axial T2-weighted MR images to identify the position of

the PRESS volumes centered at the centrum semiovale and temporal lobe. The positions of the individual voxels selected for metabolite quantification are marked on the transverse T2-weighted images. Figure 2 shows the spectroscopic images of NAA localized at the centrum semiovale (Fig 2A) and in the temporal lobe (Fig 2B) of a young participant. Also shown (Fig 2C) are four representative ^{1}H MR spectra, selected from the cortical, semioval, hippocampal, and temporal regions, to illustrate the regional variations (location and nominal size of individual voxel are indicated in the corresponding MRS images).

Metabolite Changes with Aging

Metabolite ratios of %NAA, NAA:Cho, and NAA:Cr were significantly decreased with aging in the cortical, semioval, and temporal regions. In contrast, %Cho and %Cr ratios were significantly increased during aging in the same brain regions with the exception of the %Cr ratio in the temporal region. Rates (in percent per decade) and correlation coefficients of the linear regressions, calculated for each cerebral region between the metabolite measures and the age of the participants, are listed

TABLE 1: Rates (in % of decade) and correlation coefficients (r) of the linear regressions calculated between the metabolite ratios in four cerebral regions and the age of the subjects

Regions	%NAA	%Cho	%Cr	NAA/Cho	NAA/Cr	Cho/Cr
Cortical	−2.15**	3.37*	3.86**	−4.3*	−4.6**	−0.22
	(0.56)	(0.43)	(0.56)	(0.49)	(0.59)	(0.03)
Semioval	−2.81***	5.34*	3.54*	−5.73**	−4.96**	1.44
	(0.63)	(0.49)	(0.47)	(0.56)	(0.61)	(0.14)
Temporal	−2.50**	4.95**	2.82	−5.89	−4.04*	2.26
	(0.58)	(0.49)	(0.27)	(0.53)	(0.38)	(0.15)
Hippocampal	−1.39	2.02	1.36	−2.96	−2.53	0.76
	(0.35)	(0.29)	(0.14)	(0.33)	(0.23)	(0.06)

Note.—Significance of correlation coefficients: * $P < .01$, ** $P < .001$, *** $P < .0001$.
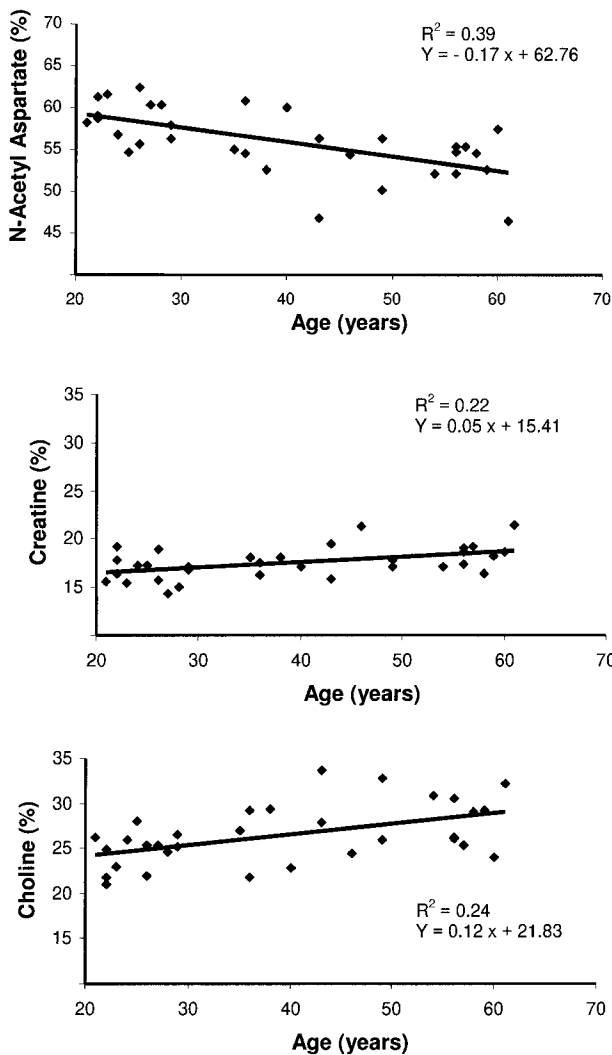

FIG 3. Regression plots of %NAA, %Cr, and %Cho in the semioval region regarding age.

in Table 1. The scatter plots shown in Figure 3 illustrate the relationship of the metabolite percentages (NAA, Cr, and Cho) in the semioval region with respect to age.

Based on a cluster analysis, a significant metabolic difference was found between two groups of 16 participants ranging in age from 21 to 39 years (younger group) and 40 to 61 years (older group).

Metabolite ratios obtained from cortical, semioval, temporal, and hippocampal regions are listed in Table 2 for both age groups. Repeated measures analysis of variance yielded significant group differences, with the effect of age being significant ($P < .05$) for all metabolite measures except the Cho:Cr ratio and the regional effect being significant ($P < .0001$) for all measures. The interaction group was not significant for any measures. Metabolite measures were then compared between the two age groups by using a multiple comparison procedure (Bonferroni's correction) to adjust for regional differences. %NAA ($P < .001$) and ratios of NAA: Cho and NAA:Cr ($P < .01$) were significantly decreased in the semioval and temporal regions of the older group compared with the younger group.

Regional Metabolite Differences

When compared with other regions, %NAA and %Cho ratios were significantly lower in the hippocampal and cortical regions, respectively. In contrast, %Cr ratio was significantly higher in the cortical and hippocampal regions compared with the semioval and temporal regions. Consequently, NAA:Cho and NAA:Cr ratios were significantly decreased in the hippocampal region compared with the other cerebral regions. Cho:Cr ratio was significantly higher in the semioval and temporal regions than in the cortical region.

Gender Differences

The metabolite measures obtained from each brain region showed no differences between the male and female groups. Therefore, data for both genders were combined for all regions.

Discussion

The major findings in these experiments were significant differences in regional metabolite levels and significant changes in metabolite ratios with advancing age of the normal participants.

Regional Metabolic Differences

Regional analysis showed that metabolite distribution varied among different brain regions.

TABLE 2: Metabolite ratios (Mean ± SD) in four cerebral regions and two age groups

Regions	Age Group	%NAA	%Cho	%Cr	NAA/Cho	NAA/Cr	Cho/Cr
Cortical	Y	58 ± 3	23 ± 2	19 ± 2	2.59 ± 0.31	3.08 ± 0.38	1.19 ± 0.11
	O	55 ± 3	24 ± 3	20 ± 1	2.28 ± 0.36	2.71 ± 0.29	1.20 ± 0.13
Semioval	Y	58 ± 3	25 ± 3	17 ± 1	2.34 ± 0.35	3.46 ± 0.40	1.50 ± 0.19
	O	54 ± 4**	28 ± 3	18 ± 2	1.95 ± 0.36*	2.96 ± 0.37*	1.54 ± 0.23
Temporal	Y	59 ± 4	24 ± 4	16 ± 2	2.50 ± 0.54	3.68 ± 0.53	1.51 ± 0.31
	O	55 ± 3**	27 ± 2	18 ± 2	2.07 ± 0.20*	3.13 ± 0.58*	1.52 ± 0.27
Hippocampal	Y	55 ± 3	26 ± 2	19 ± 3	2.11 ± 0.27	2.95 ± 0.51	1.41 ± 0.27
	O	52 ± 3	28 ± 3	20 ± 2	1.91 ± 0.29	2.68 ± 0.44	1.43 ± 0.26

* $P < .01$ and ** $P < .001$ when the older (40–61 y) groups are compared with the younger (20–39 y) groups with repeated measure analysis of variance and Bonferroni's correction for the four regions.

%NAA ratio was significantly lower in the hippocampal region when compared with other regions. This finding is consistent with those of several previous reports (20, 39, 40), including a recent quantitative MRS study localized on the hippocampus (41). Low NAA in hippocampus is in good agreement with reduced neuronal densities reported for the hippocampus and parahippocampal gyrus from embryologic and histologic evidence (42). Studies of cell type-specific cultures revealed that Cho concentration in astrocytes or oligodendrocytes was greater than in neurons (24). Thus, the most likely explanation for the high Cho content in the hippocampal region is an increased glial cell density relative to the cerebrum. This hypothesis is consistent with our finding of higher %Cho in white matter tissue of the semioval and temporal regions compared with the cortical region. Other ^{1}H MRS investigations of regional distribution were performed mostly in the frontoparietal brain gray matter and white matter and reported a significant variability in the gray matter:white matter ratio of NAA and Cho metabolites (18, 19, 25, 28–30, 43–46). However, there is a general agreement indicating a higher Cr concentration in gray matter than in white matter, which is consistent with our finding of higher %Cr ratio in the cortical region. One possible explanation of these variable results is that the T_2 of NAA is longer in white matter than in gray matter, although there are conflicting results regarding regional variations in metabolite T_2 in the literature (33, 47). Therefore, our results are in good agreement with previous findings and emphasize that regional effects must be accounted for in any comparison of brain metabolites between different groups of participants. Thus, repeated measures analysis of variance was applied to test the effect of age for each metabolite measure in different brain regions.

Metabolic Changes with Aging

The second major finding of this study was that normal aging was associated with significant changes in metabolite levels relative to each brain region. First, NAA ratios were significantly decreased with aging in the cortical, semioval, and temporal regions. Possible explanations for the reduced NAA levels are diminished neuronal density and/or neuronal loss in the aged brain. NAA is considered as a major marker of neuronal cell population for several reasons. First, NAA has been shown to be significantly reduced in brain diseases, including specific neuronal injury such as epilepsy, stroke, and dementia (39, 48, 49) but also in distant metabolic depression such as diaschisis (50). Second, NAA is primarily found in neurons of mature brain (51, 52). An alternative explanation for reduced NAA levels is a diminished concentration of NAA in neurons, which may be a marker of neuronal dysfunction. Several ^{1}H MRS studies reported reversible NAA levels under conditions of functional stress (53) and in metabolic remission occurring in cases of multiple sclerosis or encephalopathies (26, 54). The reduction of NAA with aging (2.5% per decade) is consistent with histologic evidence of neuronal loss (55), volumetric MR imaging measurements of decreased gray matter (25, 56), and neuronal dysfunction due to disturbed mechanisms of plasticity (4). Further, the reduction of NAA ratios is occurring during the middle age period in agreement with the brain volume decrease reported in men older than 40 years (5). Thus, our results are in general agreement with histologic, anatomic, and spectroscopic findings (15, 16, 18, 25, 30).

In contrast to NAA, Cho content increased with aging, which is in agreement with previous reports (17, 28, 30, 57, 58). Cho MR spectroscopic signal comprises compounds that contribute to the synthesis and breakdown of Cho-containing phospholipids, such as phosphorylcholine and glycerophosphorylcholine. Elevated Cho signal was observed in many conditions associated with increased cell membrane turnover or breakdown, such as brain tumors (21) and multiple sclerosis (26). Thus, these results may reflect an increased release of Cho compounds related to membrane breakdown in the aging process. This explanation coincides with the decrease of phosphatidylcholine content observed by in vitro studies (59), and the increase of sphingomyelin synthesis with aging (60).

Although the importance of the Cr peak in the diagnosis of neurologic disorders is unclear, its in-

crease with aging was also determined by others (17, 19, 30) and corresponds to the previous observation of an increasing phosphocreatine:total phosphorous signal ratio with aging (27). Cr content provides information regarding cell energy metabolism and is associated with the degree of cell viability. Age-related %Cr increase and NAA:Cr decrease could be explained by the increase in glial cell numbers observed in the frontal, parietal, and temporal lobes (3) because they act as a source of Cr signal but not NAA signal (61).

Technical Limitations

The major limitation of this study is that tissue segmentation was not performed to correct the metabolic measures for partial volume effects. The coarse spatial resolution of ^{1}H MRS imaging may have resulted in signal averaging of different structures or tissues. With the exception of the voxels selected in the semioval region, which can be considered as "pure" white matter constitution, the voxels obtained from the cortical, temporal, and hippocampal regions are composed of different amounts of white and gray matter and CSF. Thus, our comparison between tissue types is limited. Furthermore, the voxels selected in the hippocampal region may reflect signal from hippocampus and extra-hippocampal tissue, such as the entorhinal cortex, the parahippocampal gyrus, or temporal white matter. Because hippocampus is a long and narrow structure surrounded by CSF, the final voxel volume ($1 \times 1 \times 2$ cm^3) may be approximately composed of 50% hippocampus, 35% extra-hippocampal tissue, and 15% CSF. Although the contribution of CSF to the voxel should not affect the metabolite ratios, the decline of NAA ratios may also reflect neuronal loss outside the hippocampus or even a change in tissue composition rather than in neuronal metabolism. Thus, new sequences with fast encoding and short echo times may be useful to improve the spatial resolution of ^{1}H MRS imaging and better characterize small cerebral structures (62).

There are several other limitations to the present study. First, metabolite measures were performed in several regions of the brain that are more or less sensitive to various technical difficulties. In the cortical region, metabolic measurements were performed by associating the PRESS sequence to select the signal from the brain and the water-eliminated Fourier transform sequence efficiently to suppress the extracranial lipid signal. As shown by the quality of the spectra selected in this region (Fig 2C), the lipid signal was efficiently suppressed. However, metabolite quantification may have been affected by less homogeneity of B0 and/or B1 fields in this region. In the hippocampal region, high magnetic susceptibility effects may increase the measurement variability, which can explain the absence of significant changes with aging. Nevertheless, this finding is consistent with the absence of

hippocampus atrophy during this early period of age, as shown by volumetric MR imaging (63). In contrast, measurements obtained from the semioval region should benefit from a good homogeneity of both static and RF fields and therefore may serve as a reference for the result analysis. Second, metabolite levels are reported as relative and not absolute values. It is therefore possible that aging is associated only with the increase of Cho and/or Cr whereas NAA remains constant, as reported by absolute quantification studies (19, 28, 29). Whereas quantitative ^{1}H MRS imaging is essential to individually interpret the metabolite changes occurring with aging, it is still sensitive to possible B1 field inhomogeneities or reference variations, which may increase the measurement variability. In contrast, the use of metabolite ratios reduces systematic errors due to technical imperfections described above, because it would affect all metabolite resonances for a particular voxel in the same proportion. Third, the use of a DSA technique to reduce the residual water signal modifies the intensity of metabolite peaks by different amounts as we move away from the center frequency. The corrected measurements reported in Table 1 are consistent with those of previous reports of MR spectroscopic studies of brain (15, 30, 64).

Conclusion

Despite these limitations, this study shows that the aging process is characterized by metabolic changes that start during the middle age period. The diminished NAA content and the increased Cho and Cr contents suggest that brain aging is characterized by a reduction in neuronal viability or function associated with an accelerated membrane degradation and/or an increase in glial cell numbers. Therefore, age effects must be considered in ^{1}H MRS imaging studies of human brain diseases and careful age matching should be made between study groups. Furthermore, because the reductions of NAA ratios are considered to reflect neuronal alteration or dysfunction, ^{1}H MRS imaging studies may provide stronger support for neuronal damage than volumetric MR imaging studies. These methods may provide a better tool for the characterization and diagnosis of neurodegenerative processes such as Alzheimer disease (65).

References

1. Von Dras DD, Blumenthal HT. **Dementia of the aged: disease or atypical-accelerated aging? biopathological and psychological perspectives.** *J Am Geriatr Soc* 1992;40:285–294
2. Mrak RE, Griffin ST, Graham DI. **Aging-associated changes in human brain.** *J Neuropathol Exp Neurol* 1997;56:1269–1275

3. Terry RD, DeTeresa R, Hansen LA. **Neocortical cell counts in normal human adult aging.** *Ann Neurol* 1987;21:530–539

4. Hatanpaa K, Isaacs KR, Shirao T, Brady DR, Rapoport SI. **Loss of proteins regulating synaptic plasticity in normal aging of the human brain and in Alzheimer disease.** *J Neuropathol Exp Neurol* 1999;58:637–643

5. Double KL, Halliday GM, Kril JJ, et al. **Topography of brain atrophy during normal aging and Alzheimer's disease.** *Neurobiol Aging* 1996;17:513–521

6. Raz N, Gunning FM, Head D, et al. **Selective aging of the human cerebral cortex observed in vivo: differential vulnerability of the prefrontal gray matter.** *Cerebral Cortex* 1997;7:268–282

7. Lim KO, Zipursky RB, Watts MC, Pfefferbaum A. **Decreased gray matter in normal aging: an in vivo magnetic resonance study.** *J Gerontol* 1992;47:b26–b30

8. Guttmann CRG, Killiany RJ, Moss MB, Sandor T, Albert MS, Jolesz FA. **White matter changes with normal aging.** *Neurobiology* 1998;50:972–978

9. Almkvist O, Wahlund L-O, Andersson-Lundman G, Basun H, Backman J. **White matter hyperintensity and neuropsychological functions in dementia and healthy aging.** *Arch Neurol* 1992; 49:626–632

10. Rao SM, Mittenberg W, Bernardin L, Haughton V, Leo GJ. **Neurological test findings in subjects with leukoariosis.** *Arch Neurol* 1997;49:40–44

11. Leenders KL, Perani D, Lammertsma AA, et al. **Cerebral blood flow, blood volume and oxygen utilization: normal values and effect of age.** *Brain* 1990;113:27–47

12. Meyer JS, Terayama Y, Takashima S. **Cerebral circulation in the elderly.** *Cereb Brain Metab Rev* 1993;5:122–146

13. Pantano P, Baron J-C, Lebrun-Grandié P, Duquesnoy N, Bousser M-G, Comar D. **Regional cerebral blood flow oxygen consumption in human aging.** *Stroke* 1984;15:635–641

14. Loessner A, Alavi A, Lewandrowski KU, Mozley D, Souder E, Gur RE. **Regional cerebral function determined by FDG-PET in healthy volunteers: normal patterns and changes with age.** *J Nucl Med* 1995;36:1141–1149

15. Christiansen P, Toft P, Larsson HBW, Stubgaard M, Henriksen O. **The concentration of N-acetyl aspartate, creatine + phophocreatine, and choline in different parts of the brain in adulthood and senium.** *Magn Reson Imaging* 1993;11:799–806

16. Fukuzako H, Hashiguchi T, Sakamoto Y, et al. **Metabolite changes with age measured by proton magnetic resonance spectroscopy in normal subjects.** *Psychiatry Clin Neurosci* 1997;51: 261–263

17. Chang L, Ernst T, Poland RE, Jenden DJ. **In vivo proton magnetic resonance spectroscopy of the normal aging human brain.** *Life Sci* 1996;58:2049–2056

18. Charles CH, Lazeyras F, Krishnan KRR, et al. **Proton spectroscopy of human brain: effects of age and sex.** *Prog Neuropsychopharmacol Biol Psychiatry* 1994;18:995–1004

19. Saunders DE, Howe FA, van den Boogaart A, Griffiths JR, Brown MM. **Aging of the adult human brain: in vivo quantification of metabolite content with proton magnetic resonance spectroscopy.** *J Magn Reson Imaging* 1999;9:711–716

20. Connelly A, Jackson GD, Duncan JS, King MD, Gadian DG. **Magnetic resonance spectroscopy in temporal lobe epilepsy.** *Neurology* 1994;44:1411–1417

21. Preul MC, Caramanos Z, Collins DL, et al. **Accurate, noninvasive diagnosis of human brain tumors by using proton magnetic resonance spectroscopy.** *Nat Med* 1996;2:323–325

22. Graham GD, Blamire AM, Rothman DL, et al. **Early temporal variation of cerebral metabolites after human stroke: a proton magnetic resonance spectroscopy study.** *Stroke* 1993;24: 1891–1896

23. Kwo-On-Yuen PF, Newmark RD, Budinger TF, Kaye JA, Ball MJ, Jagust WJ. **Brain N-acetyl-L-aspartic acid in Alzheimer's disease: a proton magnetic resonance spectroscopy study.** *Brain Res* 1994;667:167–174

24. Urenjak J, Williams RJ, Gadian DG, Noble M. **Proton nuclear magnetic resonance spectroscopy unambiguously identifies different neural cell types.** *J Neurosci* 1993;13:981–989

25. Lim KO, Spielman DM. **Estimating NAA in cortical gray matter with applications for measuring changes due to aging.** *Magn Reson Med* 1997;37:372–377

26. DeStefano N, Matthews PM, Fu L,et al. **Axonal damage correlates with disability in patients with relapsing-remitting multiple sclerosis: results of a longitudinal magnetic resonance spectroscopy study.** *Brain* 1998;121:1469–1477

27. Longo R, Ricci C, Dalla Palma L, et al. **Quantitative 31P MRS of the normal adult human brain: assessment of interindividual differences and ageing effects.** *NMR Biomed* 1993;6:53–57

28. Soher BJ, Van Zijl PCM, Duyn JH, Barker PB. **Quantitative proton MR spectroscopic imaging of the human brain.** *Magn Reson Med* 1996;35:356–363

29. Pfefferbaum A, Adalsteinsson E, Spielman D, Sullivan EV, Lim KO. **In vivo spectroscopic quantification of the N-acetyl moiety, creatine, and choline from large volumes of brain gray and white matter: effects of normal aging.** *Magn Reson Med* 1999;41:276–284

30. Lundbom N, Barnett A, Bonavita S, et al. **MR image segmentation and tissue metabolite contrast in ¹H spectroscopic imaging of normal and aging brain.** *Magn Reson Med* 1999;41: 841–845

31. Tedeschi G, Bertolino A, Righini A, et al. **Brain regional distribution pattern of metabolite signal intensities in young adults by proton magnetic resonance spectroscopic imaging.** *Neurology* 1995;45:1384–1391

32. Pouwels PJW, Frahm J. **Regional metabolite concentrations in human brain as determined by quantitative localized proton MRS.** *Magn Reson Med* 1998;39:53–60

33. Frahm J, Bruhn H, Gyngell ML, Merbolt KD, Hänicke W, Sauter R. **Localized proton NMR spectroscopy in different regions of the human brain in vivo: relaxation times and concentrations of cerebral metabolites.** *Magn Reson Med* 1989;11:47–63

34. Folstein MF, Folstein SE, McHugh PR. " **Mini-Mental State": a practical method for grading the cognitive state of patients for the clinician.** *J Psychiatr Res* 1975;12:189–198

35. Patt SL, Sykes BD. **T1 water eliminated Fourier transform NMR spectroscopy.** *J Chem Phys* 1972;55:3182–3184

36. Den Hollander JA, Oosterwaal B, Van Vroonhoven H, Luyten PR. **Elimination of magnetic field distortions in ¹H NMR spectroscopic imaging.** Presented at the Annual Meeting of the Society of Magnetic Resonance in Medicine, San Francisco, August 1991

37. Roth K, Kimber BJ, Feeney J. **Data shift accumulation and alternate delay accumulation techniques for overcoming dynamic range problems.** *J Magn Reson* 1980;41:302–304

38. Tou JT, Gonzalez RC. *Pattern Recognition Principles.* Reading, Ma: Addison-Wesley;1974

39. Hugg JW, Laxer KD, Matson GB, et al. **Neuronal loss localizes human temporal lobe epilepsy by in vivo proton magnetic resonance spectroscopic imaging.** *Ann Neurol* 1993;34:788–794

40. Breiter SN, Arroyo S, Mathews VP, Lesser RP, Bryan RN, Barker PB. **Proton MR spectroscopy in patients with seizure disorder.** *AJNR Am J Neuroradiol* 1994;15:373–384

41. Choi CG, Frahm J. **Localized proton MRS of the human hippocampus: metabolite concentrations and relaxation times.** *Magn Reson Med* 1999;41:204–207

42. Arnold SE, Trojanowski JQ. **Human fetal hippocampal development: I. cytoarchitecture, myeloarchitecture, and neuronal morphologic features.** *J Comp Neurol* 1996;376:274–292

43. Doyle TJ, Bedell BJ, Narayama PA. **Relative concentrations of proton MR visible neurochemicals in gray and white matter in human brain.** *Magn Reson Med* 1995;33:755–759

44. Wang Y, Li SJ. **Differentiation of metabolic concentrations between gray matter and white matter of human brain by in vivo ¹H magnetic resonance spectroscopy.** *Magn Reson Med* 1998;39:28–33

45. Duc CO, Weber OM, Trabesinger AH, Meier D, Boesiger P. **Quantitative ¹H MRS of the human brain in vivo based on the simulation phantom calibration strategy.** *Magn Reson Med* 1998;39:491–496

46. Pan JW, Twieg DB, Hetherington HP. **Quantitative spectroscopic imaging of the human brain.** *Magn Reson Med* 1998;40: 363–369

47. Hetherington HP, Mason GF, Pan JW, et al. **Evaluation of cerebral gray and white matter metabolite differences by spectroscopic imaging at 4.1T.** *Magn Reson Med* 1994;32:565–571

48. Sappey-Marinier D, Calabrese G, Hetherington HP, et al. **Proton magnetic resonance spectroscopy of human brain: application to normal white matter, chronic infarction, and MRI white matter signal hyperintensities.** *Magn Reson Med* 1991;26: 313–327

49. Meyerhoff DJ, Mac Kay S, Constans JM, et al. **Axonal injury and membrane alterations in Alzheimer's disease suggested by in vivo proton magnetic resonance spectroscopic imaging.** *Ann Neurol* 1994;36:40–47

50. Fulham MJ, Dietz MJ, Duyn JH. **Transsynaptic reduction in N-acetylaspartate in cerebellar diaschisis: a proton MR spectroscopic imaging study.** *J Comput Assist Tomogr* 1994;18:697–704

51. Moffset JR, Namboori MA, Cangro CB, Neale JH. **Immunohistochemical localization of N-acetylaspartate in rat brain.** *Neuroreport* 1991;2:131–134

52. Miller B. **A review of chemical issues in ¹H NMR spectroscopy: N-Acetyl-L-aspartate, creatine and choline.** *NMR Biomed* 1991; 4:47–52

53. Taylor DL, Davies SE, Obrenovitch TP, et al. **Investigation into the role of N-acetylaspartate in cerebral osmoregulation.** *J Neurochem* 1995;65:275–281

54. Vion-Dury J, Confort-Gouny S, Nicoli F, et al. **Localized brain proton MRS metabolic patterns in HIV-related encephalopathies.** *C R Acad Sci III* 1994;317:833–840

55. Simic G, Kostovic I, Winblad B, Bogdanovic N. **Volume and number of neurons of the human hippocampal formation in normal aging and Alzheimer's disease.** *J Comp Neurol* 1997; 379:482–494

56. Matsumae M, Kikinis R, Morocz I, et al. **Age-related changes in intracranial compartment volumes in normal adults assessed by magnetic resonance.** *J Neurosurg* 1996;84:982–991

57. Kreis R, Ernst T, Ross BD. **Development of human brain: in vivo quantification of metabolite and water content with proton magnetic resonance spectroscopy.** *Magn Reson Med* 1993; 30:424–437

58. Moats RA, Ernst T, Shonk TK, Ross BD. **Abnormal cerebral metabolite concentrations in patients with probable Alzheimer disease.** *Magn Reson Imag* 1994;32:110–115

59. Rouser G, Yamamoto A. **Curvilinear regression course of human brain lipid composition changes with age.** *Lipids* 1998;3: 284–287

60. Giusto NM, Roque ME, Ilincheta de Bochero MG. **Effect of aging on the content, composition and synthesis of sphingomyelin in the central nervous system.** *Lipids* 1992;27:835–839

61. Birken DL, Oldendorf WH. **N-acetyl-L-aspartic acid: a literature review of a compound prominent in ¹H-NMR spectroscopic studies of brain.** *Neuro Behav Rev* 1989;13:23–31

62. Wiedermann D, Schuff N, Matson G, Soher B, Maudsley AA, Weiner MW. **Test-reliability of short multislice ¹H MRSI.** Presented at the Annual Meeting of the International Society for Magnetic Resonance in Medicine, Denver, April 2000

63. Sullivan EV, Marsh L, Mathalon DH, Lim KO, Pfefferbaum A. **Age-decline in MRI volumes of temporal lobe gray matter but not hippocampus.** *Neurobiol Aging* 1995;16:591–606

64. Constans JM, Meyerhoff DJ, Gerson J, et al. **H-1 MR spectroscopic imaging of white matter signal hyperintensities: Alzheimer disease and ischemic vascular dementia.** *Radiology* 1995;197:517–523

65. Schuff N, Amend D, Ezekiel F, et al. **Changes of hippocampal N-acetyl aspartate and volume in Alzheimer's disease.** *Neurology* 1997;49:1513–1521